



**TiCl<sub>4</sub>-promoted Condensation of Methyl Acetoacetate,  
Isobutyraldehyde, and Indole: A Theoretical and  
Experimental Study**

Journal:	<i>Physical Chemistry Chemical Physics</i>
Manuscript ID:	CP-ART-11-2014-005412.R2
Article Type:	Paper
Date Submitted by the Author:	19-Feb-2015
Complete List of Authors:	Renzetti, Andrea; Osaka City University, Department of Chemistry Marrone, Alessandro; Università "G. d'Annunzio" di Chieti-Pescara, Dipartimento di Farmacia Gérard, Stéphane; Université de Reims Champagne-Ardenne, Département de Chimie Organique Pharmaceutique Sapi, Janos; Université de Reims Champagne-Ardenne, Département de Chimie Organique Pharmaceutique Nakazawa, Hiroshi; Osaka City University, Department of Chemistry Re, Nazzareno; Università "G. d'Annunzio" di Chieti-Pescara, Dipartimento di Farmacia Fontana, Antonella; Università "G. d'Annunzio" di Chieti-Pescara, Dipartimento di Farmacia

## ARTICLE

# TiCl<sub>4</sub>-promoted Condensation of Methyl Acetoacetate, Isobutyraldehyde, and Indole: A Theoretical and Experimental Study

Cite this: DOI: 10.1039/x0xx00000x

Received 00th January 2012,  
Accepted 00th January 2012

DOI: 10.1039/x0xx00000x

www.rsc.org/

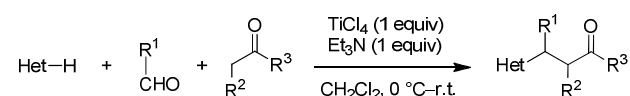
Andrea Renzetti,<sup>\*a†</sup> Alessandro Marrone,<sup>\*b†</sup> Stéphane Gérard,<sup>c</sup> Janos Sapi,<sup>c</sup> Hiroshi Nakazawa,<sup>a</sup> Nazzareno Re,<sup>b</sup> and Antonella Fontana<sup>b</sup>

The mechanism of the TiCl<sub>4</sub>-promoted condensation of methyl acetoacetate, isobutyraldehyde, and indole was studied by a combination of theoretical and experimental techniques. The energy profile of plausible reaction paths was evaluated by DFT calculations, and various reaction intermediates were isolated or observed in solution by NMR spectroscopy. Theoretical and experimental results indicate that the reaction proceeds in three steps, all promoted by titanium: 1) formation of the enolate ion of methyl acetoacetate, 2) Knoevenagel condensation of enolate ion and aldehyde, and 3) Michael addition of indole to the Knoevenagel adduct. The study sheds light on the role of titanium in the reaction, providing a mechanistic model for analogous reactions.

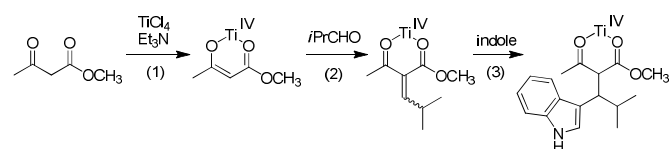
## Introduction

Multicomponent reactions are reactions where three or more molecules react to form a single product.<sup>1-3</sup> Due to the high atom economy and the large ( $\geq 3$ ) number of molecules involved, multicomponent reactions afford compounds with complex structure. They are widely used in combinatorial chemistry to synthesize libraries of compounds having a common scaffold.<sup>4,5</sup> They are also increasingly used in diversity-oriented synthesis to generate compounds with high structural diversity.<sup>6-8</sup> In this context, we have previously reported a TiCl<sub>4</sub>-promoted trimolecular condensation of aromatic heterocycles, aldehydes, and carbonyl derivatives to afford polyfunctionalized heterocycles (Scheme 1).<sup>9,10</sup> The reaction likely takes place in three steps: (1) Formation of the enolate ion, (2) Knoevenagel condensation of enolate ion and aldehyde, and (3) Michael addition of heterocycle to the Knoevenagel adduct. We have previously investigated the mechanism of steps (1) and (2) for the reaction of dimethyl malonate and three aldehydes (formaldehyde, isobutyraldehyde, and benzaldehyde) by a theoretical and experimental approach.<sup>11</sup> In this paper, the same approach was used to study the mechanism of steps (1)–(3) for the reaction of methyl acetoacetate, isobutyraldehyde, and indole (Scheme 2). The goal of this work was to gain an insight into the mechanism of the entire trimolecular process, with particular regard to the Michael addition of step (3). Although the use of Ti(IV) in Michael-type reactions has been known for almost forty years<sup>12</sup>

with important applications in organic synthesis,<sup>13-31</sup> the number of mechanistic studies on such reactions is limited.<sup>18-23,32-39</sup> This study might contribute to elucidate the trimolecular reaction as well as analogous reactions involving different substrates.



Het-H = indole, pyrrole, 2-methylfuran  
R<sup>1</sup> = *i*-Pr, Ph, (2-NO<sub>2</sub>)Ph  
R<sup>2</sup> = MeCO, PhCO, MeSO<sub>2</sub>, NO<sub>2</sub>  
R<sup>3</sup> = OMe, OEt, Me

Scheme 1. TiCl<sub>4</sub>-promoted trimolecular condensation.Scheme 2. Mechanism of TiCl<sub>4</sub>-promoted trimolecular condensation investigated in this work.

## Results and Discussion

### Formation of enolate ion

**Experimental evidence.** In agreement with previous evidence on the enolate of  $\beta$ -diesters,<sup>11</sup>  $\beta$ -phosphonoacetates,<sup>40</sup> and  $\alpha$ -alkoxyketones,<sup>41</sup> NMR spectroscopic studies confirmed the following results: (i) the formation of methyl acetoacetate–TiCl<sub>4</sub> complex upon addition of 1 molar equivalent of TiCl<sub>4</sub> to a solution of  $\beta$ -ketoester (Figure 1, compare spectra a and b; Table S1, check the change in chemical shift of  $\alpha$ -carbon signal); (ii) the formation of an O-titanium enolate upon addition of 1 molar equivalent of triethylamine (Figure 1c and Table S1, check the change in chemical shift, multiplicity, and  $J$  value of  $\alpha$ -carbon signal); and (iii) the tautomerization of enolate to the deuterated ester on quenching with a solution of DCl in D<sub>2</sub>O. We further investigated the methyl acetoacetate–TiCl<sub>4</sub> complex to elucidate its structure in solution. The corresponding Job's plot<sup>42–45</sup> shows a maximum at  $\chi_{\text{TiCl}_4} = 0.503$  (Figure 2). This result indicates that the complex has a 1:1 stoichiometry at the investigated concentration<sup>46,47</sup> and temperature,<sup>48</sup> analogously to the diethyl malonate–TiCl<sub>4</sub> complex.<sup>11</sup>

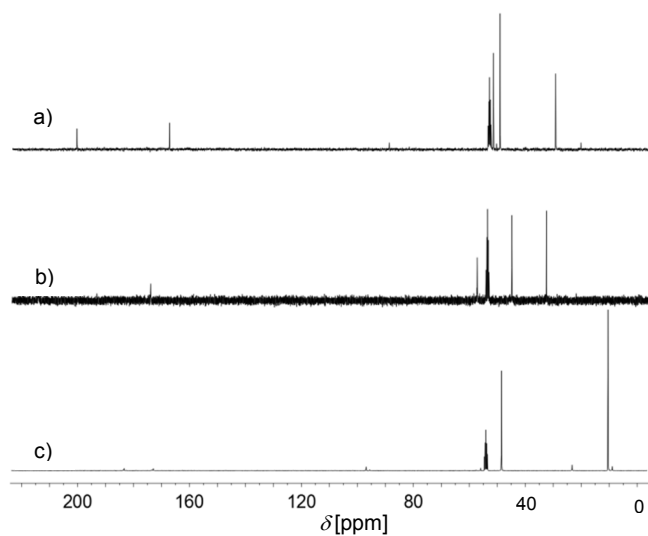


Figure 1. <sup>13</sup>C NMR spectra of methyl acetoacetate a) pure; b) after addition of TiCl<sub>4</sub> (1.0 equiv); c) after addition of TiCl<sub>4</sub> (1.0 equiv) and Et<sub>3</sub>N (1.0 equiv) (solvent: CD<sub>2</sub>Cl<sub>2</sub>, T = 25 °C).

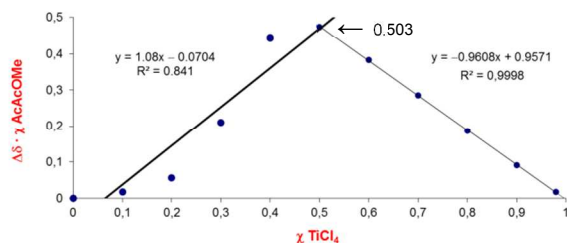


Figure 2. Job's plot for the complex methyl acetoacetate–TiCl<sub>4</sub> ( $\Delta\delta$  = chemical shift variation of the H <sub>$\alpha$</sub>  in the <sup>1</sup>H NMR spectrum,  $\chi_{\text{AcAcOMe}}$  = molar fraction of methyl acetoacetate,  $\chi_{\text{TiCl}_4}$  = molar fraction of TiCl<sub>4</sub>, [methyl acetoacetate] + [TiCl<sub>4</sub>] = 0.83 M, solvent: CDCl<sub>3</sub>, T = 25 °C).

**Theoretical calculations.** The formation of titanium enolate was investigated by DFT approach. Based on evidence above as well as previous investigation on  $\beta$ -ketoesters<sup>48</sup> and  $\beta$ -diesters,<sup>49</sup> we assumed the formation of a 1:1 complex between methyl acetoacetate and TiCl<sub>4</sub> in which both carbonyl groups are coordinated to metal (complex **1a** in Chart 1). Bi-coordinated complex **1b** and mono-coordinated complexes **1c** and **1d** were all detected  $\sim 6$  kcal mol<sup>-1</sup> higher in energy than **1a**, which is thus predominant in CH<sub>2</sub>Cl<sub>2</sub>. Deprotonation of **1a** may lead to the formation of either the anionic tetrachlorotitanium enolate **2** (Scheme 3, step I) or the neutral trichlorotitanium enolate **2'** if a chloride ion dissociates from metal (Scheme 3, step I'). Calculated free energies for the formation of titanium enolates **2** and **2'** in dichloromethane are  $-19.6$  and  $-9.4$  kcal mol<sup>-1</sup>, respectively. The anionic complex **2** is thermodynamically favored over the neutral complex **2'**, probably due to the energy required for chloride dissociation in the latter case. These results indicate that deprotonation of complex **1a** is complete and occurs through step I, affording titanium enolate **2**. Analysis of the atomic charge distribution showed that the negative charge of **2** is delocalized over the six-membered metallacycle (Table S2). The metal and ketone charge basins of **2** host each about 30% of negative charge, with the remaining 40% being placed on  $\alpha$ -carbon and ester.<sup>50</sup> Charge delocalization of **2** is consistent with hybridization change from  $sp^3$  to  $sp^2$  on passing from ester to enolate observed by <sup>13</sup>C NMR spectroscopy (Table S1).

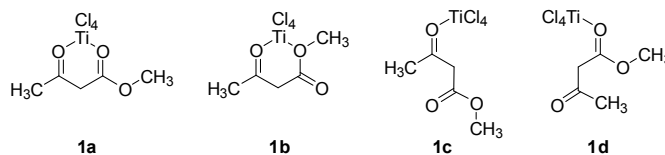
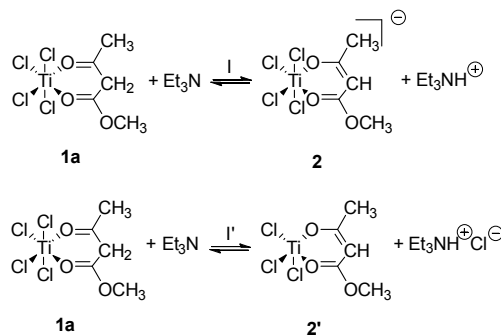


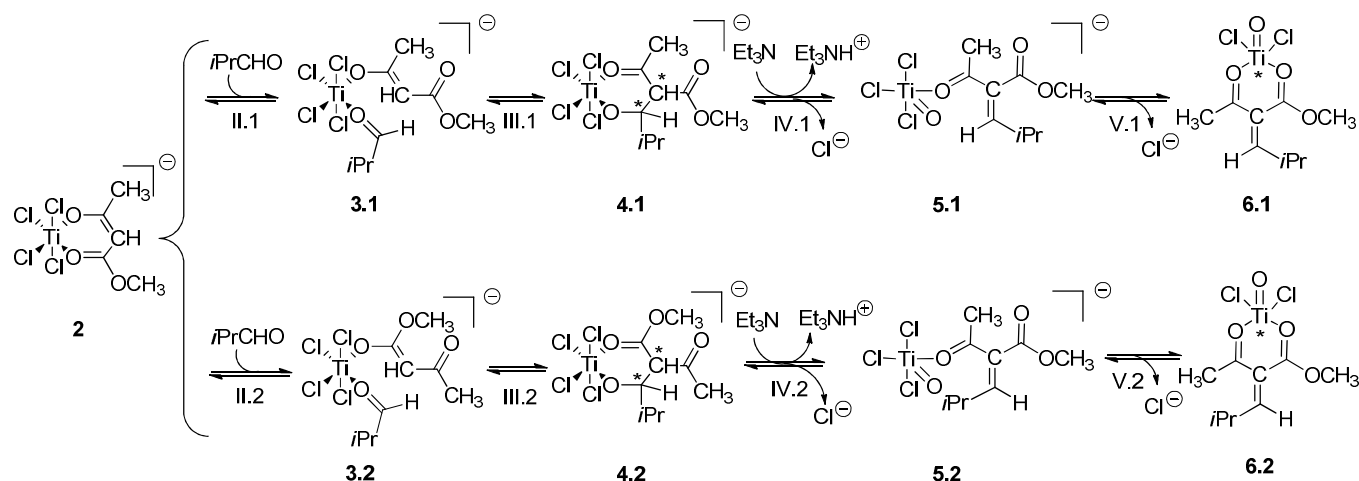
Chart 1. Possible structures for a 1:1 complex methyl acetoacetate–TiCl<sub>4</sub>.



Scheme 3. Formation of titanium enolates of methyl acetoacetate.

### Knoevenagel condensation

**Theoretical calculations.** The Knoevenagel condensation between isobutyraldehyde and methyl acetoacetate was theoretically investigated by assuming the same reaction mechanism reported for the condensation of isobutyraldehyde and dimethyl malonate (Scheme 4).<sup>11</sup> Isobutyraldehyde reacts with anionic titanium enolate **2** by replacing one of the carbonyl groups of acetoacetate in the titanium coordination. Two paths are possible depending on which carbonyl group (*i.e.*, the ester or the ketone) is replaced by aldehyde (Scheme 4, steps II.1–V.1 and II.2–V.2, respectively).



Scheme 4. Steps of the Knoevenagel condensation investigated in this work.

The aldol reaction III leads to the formation of two six-membered metallacycles (**4.1** and **4.2**). Each of them has two stereogenic centers, so eight stereoisomers (four pairs of enantiomers) may be formed in this process (Chart S1). Because two enantiomers in the same conformation have the same energy, calculations were restricted to four stereoisomers (Chart S1). In the following elimination step IV, the approach of base to  $C_{\alpha}$  is sterically favored when the geometry of **4** places the isopropyl group and the  $C_{\alpha}$ -H on different sides of the metallacycle plane. Based on the model of this reaction and of analogous asymmetric aldol reactions,<sup>51</sup> only two stereoisomers [(*2R,3S*)-**4.1** and (*2S,3S*)-**4.2**, arrowed in Chart S1] were considered in calculations of step IV.

An alternative mechanism for the Knoevenagel condensation involves the coordination of aldehyde to the neutral titanium enolate **2'**, followed by attack of the  $C_{\alpha}$  of enolate to the carbonyl carbon of aldehyde to afford a metallabicyclic intermediate. However, this mechanism was excluded because it has been shown to be kinetically disfavored in the condensation of dimethyl malonate.<sup>11</sup>

Theoretical calculations indicate that the overall condensation of methyl acetoacetate and isobutyraldehyde is a highly favored process, with reaction free energies of  $-19.3$  and  $-14.5$  kcal mol<sup>-1</sup> for the formation of **6.1** and **6.2**, respectively (Table 1). Moreover, the *Z* isomer of the free adduct is thermodynamically more stable than the *E* by  $4.7$  kcal mol<sup>-1</sup>, in agreement with the experimentally determined *E/Z* ratio of 1:1.5 (*vide infra*). Consistently with previous results,<sup>11</sup> calculations also suggest that the Knoevenagel condensation is thermodynamically controlled, as evidenced by the small activation enthalpies calculated for steps III.1, III.2, IV.1, and IV.2 (Table 1).

**Experimental evidence.** Theoretical calculations are in agreement with experimental evidence. The Knoevenagel adduct **K** of methyl acetoacetate and isobutyraldehyde was synthesized under the reaction conditions of trimolecular condensation (*i.e.*, in the presence of 1 equivalent of TiCl<sub>4</sub> and 1 equivalent of Et<sub>3</sub>N in CH<sub>2</sub>Cl<sub>2</sub> at 0 °C for 3 h).<sup>52</sup> **K** was isolated in 60% yield as a mixture of *E/Z* isomers in 1:1.5 ratio according to <sup>1</sup>H NMR analysis. The same result was obtained when the reaction was performed at room temperature,

Table 1. Reaction enthalpies and free energies, and activation enthalpies calculated for the Knoevenagel condensation in CH<sub>2</sub>Cl<sub>2</sub>. Values in kcal mol<sup>-1</sup>.

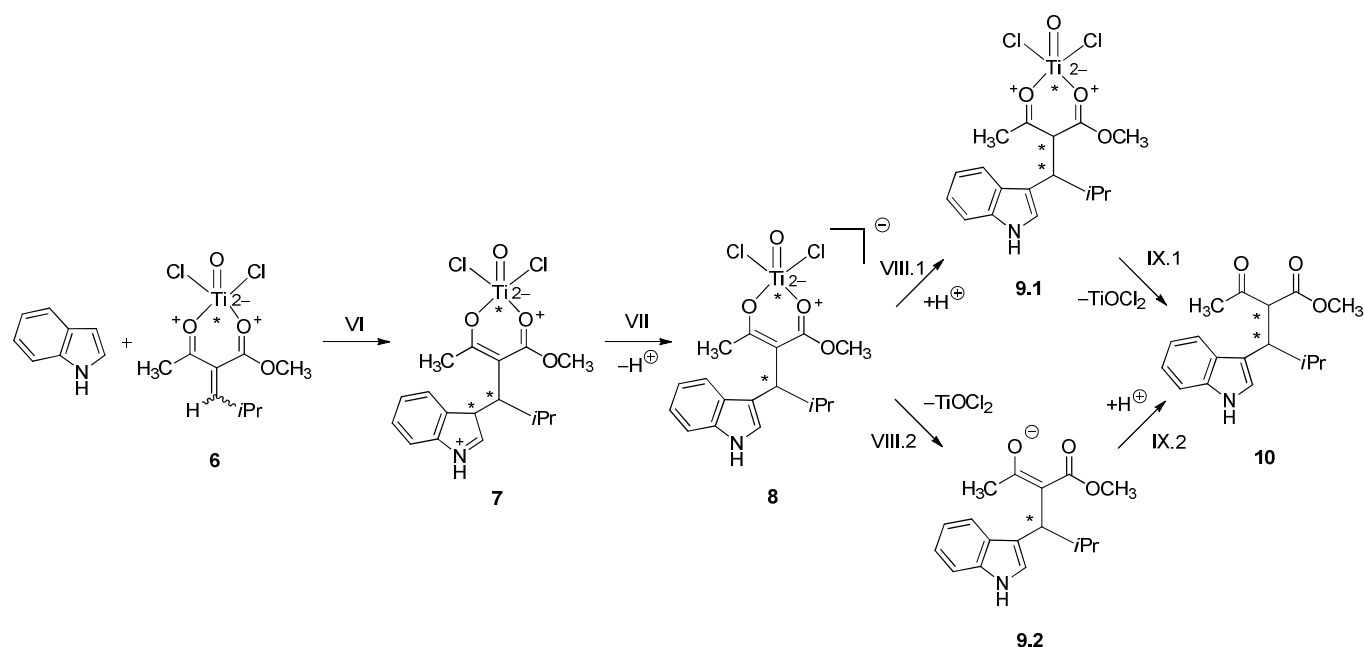
step	$\Delta H$	$\Delta G$	$\Delta H^{\ddagger}$
I	-20.1	-19.6	n.d. <sup>[a]</sup>
II.1	7.5	19.3	n.d. <sup>[a]</sup>
II.2	19.9	31.1	n.d. <sup>[a]</sup>
III.1	-1.2	0.5	17.6
III.2	-17.6	-18.0	8.5
IV.1	-13.1	-16.7	12.1
IV.2	0.3	3.8	18.0
V.1	-2.3	-2.8	n.d. <sup>[a]</sup>
V.2	-11.3	-11.9	n.d. <sup>[a]</sup>
overall 1	-29.2	-19.3	n.d. <sup>[a]</sup>
overall 2	-28.9	-14.5	n.d. <sup>[a]</sup>

[a] n.d. = not determined.

indicating that the reaction at 0 °C is also thermodynamically controlled. The two isomers were separated by column chromatography (see Experimental Section). Both (*E*)-**K** and (*Z*)-**K** isomerized in CDCl<sub>3</sub> solution affording the same mixture of *E/Z* isomers in 1:1.5 ratio. Isomerization took place spontaneously over a three-month period, and proved to be base-promoted. In the presence of 1 equivalent of Et<sub>3</sub>N in CDCl<sub>3</sub> at 20 °C, isomerization *E* ⇌ *Z* reached equilibrium after about 12 h (Figure S1).

#### Michael addition

**Theoretical calculations. Mechanistic model.** The Michael reaction between indole and Knoevenagel adduct **6** derived from methyl acetoacetate and isobutyraldehyde was theoretically investigated by DFT calculations. We considered two paths for the mechanism (Scheme 5): A (VI-VII-VIII.1-IX.1) and B (VI-VII-VIII.2-IX.2), leading to the same final product **10**. Path A includes the following steps:

Scheme 5. Mechanism of the Michael reaction between **6** and indole.

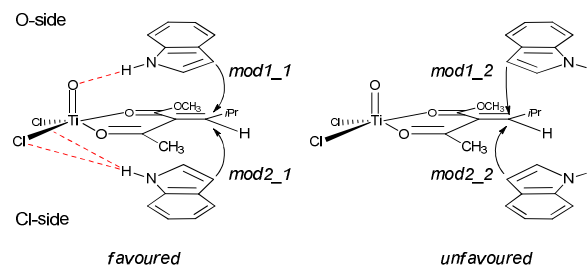
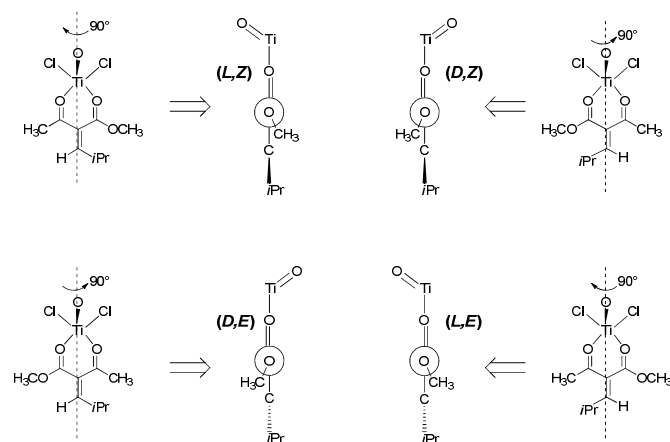
VI) Nucleophilic addition of indole to the Knoevenagel adduct-TiOCl<sub>2</sub> complex **6**, leading to the formation of intermediate **7**, VII) deprotonation of **7** by Et<sub>3</sub>N to restore the full aromaticity of indole<sup>53,54</sup> and generate the anionic intermediate **8**, VIII.1) protonation of the  $\alpha$ -carbon of **8** by Et<sub>3</sub>NH<sup>+</sup> to yield the neutral complex **9.1**, and IX.1) dissociation of TiOCl<sub>2</sub> to generate the condensation product **10**. In path B, the last two steps are inverted: firstly, **8** loses titanium generating the free enolate **9.2** (step VIII.2), then it is protonated to yield **10** (step IX.2).

Paths A and B, although affording the same final product **10**, may have a different stereochemical outcome in principle. If reaction follows path A, both stereogenic centers of titanium and C <sub>$\beta$</sub>  in **8** may induce chirality in the new stereocenter of C <sub>$\alpha$</sub>  in **9.1**. If path B is followed, chirality can be only induced by C <sub>$\beta$</sub> , because metal is removed before protonation.

Reaction of unchelated complexes **5.1** and **5.2** with indole was found to be kinetically unfeasible due to the electron-rich nature of complexes. This result allowed to rule out the formation of unchelated species in the following steps.

Michael addition starts with the attack of indole on Knoevenagel adduct-TiOCl<sub>2</sub> complex **6** (Scheme 5, step VI). The attack of C<sub>3</sub> of indole on C <sub>$\beta$</sub>  of **6** can occur on both sides of the double bond plane. For each side, several orientations of indole with respect to the Knoevenagel adduct are possible in principle. Calculations showed that the only allowed orientations, leading to local minima of the potential energy surface, are those where the N-H group of indole is oriented towards the metal (*mod1\_1* and *mod2\_1* in Scheme 6). These results indicate that the N-H group of indole donates a hydrogen bond to the oxygen atom or to the chlorine atoms of the titanil group, so that indole and the Knoevenagel adduct form a non-covalent adduct (**RA1**) before reacting. Other orientations of attack, where the N-H group of indole points far away from titanium ligands (for example *mod1\_2* and *mod2\_2* in Scheme 6), are unfavored as they are not stabilized by hydrogen bonds. Therefore, only the former two orientations of

attack were considered. The Knoevenagel adduct **6** has one stereogenic center on titanium and a C=C bond with two possible configurations (*E* and *Z*), so four stereoisomers can be drawn for this compound (Scheme 7).

Scheme 6. Possible orientations of indole attack on **6**.Scheme 7. Configurations and Newman projections for the stereoisomers of **6**.

Each of them can be attacked by indole on both sides with creation of two new stereogenic centers (Scheme 5). However, one of them is lost in step VII, so only four stereoisomers of product **8** are obtained (Scheme 5). In steps VI and VII, (*D,E*)/(*L,Z*) and (*D,Z*)/(*L,E*) couples of adduct **6** generate the same stereoisomers of **8**. Therefore, only the former couple of isomers was considered in calculations (Scheme S1). In step VIII.1, each of the four stereoisomers of **8** can be protonated on both sides of the enolate double bond plane, so eight reactions are possible for this step. Compound **9.1** has three stereogenic centers and is formed as a mixture of eight stereoisomers (four couples of enantiomers, Scheme S2). However, after removal of titanium from the reaction mixture by acidic work-up (step IX.1), one stereogenic center is lost, so in the end only four stereoisomers of the condensation product **10** are obtained.

**Thermodynamics.** Free energy profiles of steps VI–VIII.1 (Figure 3) almost parallel the corresponding enthalpy profiles (Figure 4). Therefore, the former were used to analyze the thermodynamics of these steps. In all cases, step VI resulted to be endoergonic ( $\Delta G = 11\text{--}13 \text{ kcal mol}^{-1}$ ), due to the loss of indole aromaticity. The narrow range of free energy values indicates no neat preference for the attack of indole on the O-side (red path) or the Cl-side (blue path) of the adduct. On the contrary, step VII is highly exoergonic ( $\Delta G = -27$  to  $-33 \text{ kcal mol}^{-1}$ ), as it involves the restoration of indole aromaticity. Overall, steps VI and VII lead to the highly stable enolate **8** whose formation is accompanied by a large free energy gain of  $15\text{--}21 \text{ kcal mol}^{-1}$ . Analysis of the atomic charge distribution indicates that about 45% of the negative charge in **8** is delocalized on the metal fragment  $\text{TiOCl}_2$  (Table S3). Therefore, the stability of enolate **8** is likely due to the electron-withdrawing effect of titanium, which delocalizes the negative charge of the  $\beta$ -ketoester group to the metallacycle. This result is in line with the stability of the negatively charged methyl acetoacetate enolate ion–Ti(IV) complex (**2**).

In Scheme 5, we assumed step VIII.1 takes place by direct protonation of the  $C_\alpha$  of **8** by the  $\text{Et}_3\text{NH}^+$  ion. However, delocalization of negative charge of **8** to the metal fragment suggests that protonation of **8** occurs on titanyl oxygen, not on  $C_\alpha$ . For the same reason, protonation of enolate oxygens of **8** can be ruled out. Accordingly, we considered an alternative model where reaction  $\mathbf{8} \rightarrow \mathbf{9.1}$  takes place in two steps (Scheme 8): VIII.1a) protonation of titanyl oxygen, and VIII.1b) intramolecular proton transfer from titanyl oxygen to  $C_\alpha$ . Nevertheless, according to the new model, step VIII.1 is highly endoergonic ( $16\text{--}30 \text{ kcal mol}^{-1}$ ), making the overall process  $\mathbf{6} \rightarrow \mathbf{9.1}$  highly unfavored ( $\Delta G = 25\text{--}28 \text{ kcal mol}^{-1}$ ). These free energy values correspond to an equilibrium constant  $\ll 1$ , which is not in line with the 45% yield of **10** observed experimentally.<sup>9</sup> This result indicates that the ammonium ion protonates only a small percentage of the enolate ion and suggests the participation of a stronger acid as the proton source. We concluded that protonation takes place in the aqueous phase during the final work-up by aqueous HCl. This hypothesis is reasonable as HCl is a much stronger acid than  $\text{Et}_3\text{NH}^+$  ion. Unfortunately, the protonation of enolate ion in aqueous HCl could not be modelled by using molecular or pseudo-molecular models, at least at the level of theory used in this work. The problem with modelling this type of reaction is that the final work-up yields a complex, multi-phasic mixture whose effects are poorly described by implicit solvation model. Therefore, we studied the protonation of enolate in  $\text{CH}_2\text{Cl}_2$  by replacing HCl with  $\text{CF}_3\text{COOH}$ , a strong acid soluble in organic

solvents. The acidity functions of 1 M HCl in water and 1 M  $\text{CF}_3\text{COOH}$  in  $\text{CH}_2\text{Cl}_2$  are  $-0.2^{55}$  and  $-1.6^{56}$  respectively. Thus, both compounds behave as strong acids and display comparable acidity in the respective solvents. Lower free energy values were obtained for step VIII.1 by using  $\text{CF}_3\text{COOH}$  in the place of  $\text{Et}_3\text{NH}^+$  ion. However, the use of  $\text{CF}_3\text{COOH}$  still led to positive  $\Delta G$  values ( $9\text{--}10 \text{ kcal mol}^{-1}$ ) for the reaction  $\mathbf{6} \rightarrow \mathbf{9.1}$ . These results indicate that in the absence of a final aqueous work-up, both  $C_\alpha$  protonation and metal dissociation are hampered. Consequently, the Michael reaction in dichloromethane is stopped at the formation of stable intermediate **8**.

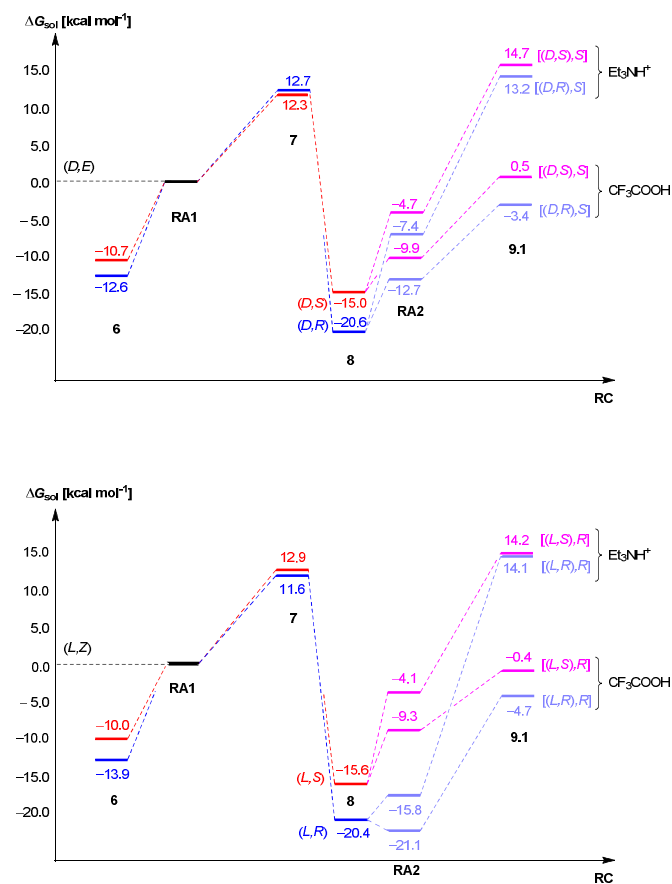
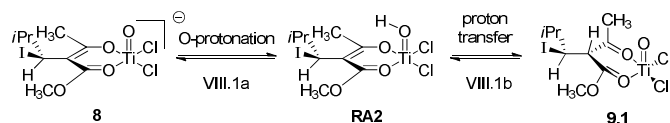


Figure 3. Calculated free energy profiles for the Michael reaction of (*D,E*)-**6** and (*L,Z*)-**6** in dichloromethane. Two reaction paths are reported: red-magenta and blue-violet, corresponding to O-side and Cl-side attack, respectively.

**Kinetics.** Step VI is slow, with activation enthalpies in the range of  $12\text{--}16 \text{ kcal mol}^{-1}$  (Figure 4), whereas step VII, involving the restoration of indole aromaticity, was found to be essentially barrierless, with activation enthalpies close to zero and within the range of computational error ( $1\text{--}2 \text{ kcal mol}^{-1}$ ).<sup>57</sup> For both (*D,E*)-**6** and (*L,Z*)-**6** adducts the attack of indole on the O-side (red path) is kinetically favored over the attack on the Cl-side (blue path), as indicated by the corresponding enthalpy barriers ( $14.2$  vs  $15.4$  and  $12.7$  vs  $14.3 \text{ kcal mol}^{-1}$ , respectively). Because step VII is highly exoergonic and almost barrierless, **7** is converted into **8** irreversibly as soon as it is formed. It ensues that the formation of **8**, as well as the involved stereochemistry, is under kinetic control. Based on this model, we used the activation enthalpies of step VI to calculate the diastereomeric

excess (d.e.) of **8**, which is a mixture of two pairs of enantiomers: *L,S/D,R* and *L,R/D,S* (see Supplementary Information). The d.e. calculated for **8** is 22%. This value is higher than that observed for the mixture of Knoevenagel adducts (*Z*)-**K** and (*E*)-**K** (20%), and shows how the preferential attack of indole on the O-side induces a slight increase in the diastereomeric yield of **8**. The result also indicates that the high (>90%) d.e. observed in the final product **10**<sup>9</sup> is likely generated in the final reaction work-up, when the enolate is protonated on C<sub>α</sub>.

**Calculations for path A.** Step VIII.1 involves protonation of titanyl oxygen followed by intramolecular proton transfer from oxygen to C<sub>α</sub> (Scheme 8). Because proton comes from titanyl group, it may only attack one side of the C<sub>α</sub> *sp*<sup>2</sup> plane, thus making step VIII.1 stereospecific. Hence, starting from two pairs of enantiomers of **8** (*D,S/L,R* and *D,R/L,S*), step VIII.1 only affords two pairs of enantiomers of **9.1**, i.e. *D,S,S/L,R,R* and *D,R,S/L,S,R* (Schemes 5 and 8). Calculations performed on a reduced model (Chart S2) indicated that protonation of titanyl oxygen (step VIII.1a) is much faster than intramolecular proton transfer (step VIII.1b) ( $\Delta H^\ddagger = 5.8$  and 18–22 kcal mol<sup>-1</sup>, respectively). Therefore, proton transfer VIII.1b is the rate-limiting step for the reaction **8**→**9.1**. This finding is in line with the well-established evidence that the slow step in keto-enol tautomerization reactions (both base- and acid-catalyzed) is the proton transfer from or to the C<sub>α</sub>, as it involves a reorganization of C<sub>α</sub> hybridization.<sup>58</sup> Step VIII.1 turned out to be the rate-determining step of the overall reaction **6**→**9.1**, with activation enthalpies of 18–23 kcal mol<sup>-1</sup> (Figure 4).<sup>59</sup> Assuming a kinetic control (short reaction time) and 100% yield for step VIII.1, the d.e. of **9.1** can be calculated analogously to **8**. Although step VIII.1 is endoergic in dichloromethane, it is expected to be spontaneous and complete in aqueous HCl, despite HCl being a weaker acid than CF<sub>3</sub>COOH in CH<sub>2</sub>Cl<sub>2</sub>, due to the high oxophilicity of titanyl group.<sup>60–63</sup> Calculations indicate that the d.e. increases from 22 to 99% on passing from **8** to **9.1**, with the *D,R,S/L,S,R* pair being widely prevalent (see Supplementary Information).



Scheme 8. Two-step mechanism for the reaction **8**→**9.1**. I = 1*H*-indol-3-yl.

**Calculations for path B.** In path B, dissociation of TiOCl<sub>2</sub> from **8** affords the free enolate **9.2** (Scheme 5, step VIII.2). **9.2** is protonated into enol, which eventually tautomerizes to the keto form **10** (Scheme 5, step IX.2). If reaction follows path B, the high d.e. observed for product **10** can be explained in two ways. One possibility is that the stereogenic center on C<sub>β</sub> of **9.2** induces chirality on the C<sub>α</sub>. Another possibility is that diastereoselectivity is induced by crystallization.<sup>64,65</sup> The condensation product bears an enolizable hydrogen on the α-carbon, so the two diastereomers may interconvert via enolization. If one diastereomer crystallizes, it is subtracted from the reaction mixture, and the interconversion equilibrium is continuously displaced towards the crystalline form until the whole compound is present as one pure diastereomer (crystallization-induced diastereoselectivity). Based on this

model, diastereoselectivity is due to the intrinsic solubility properties of the product, and is not controlled by the chirality of other centers in the molecule. The hypothesis of diastereomeric interconversion is supported by the evidence that some active methylene compounds such as α-nitroketones<sup>66</sup> have an enantiomerization barrier low enough to allow a rapid inversion of their stereogenic center at room temperature. Crystallization-induced asymmetric transformation of covalent diastereomers has been reported in several reactions,<sup>67,68</sup> including multicomponent reactions.<sup>69,70</sup> To verify this hypothesis, the kinetic barrier for the α-carbon epimerization of **10** in CHCl<sub>3</sub> catalyzed by Et<sub>3</sub>N was theoretically estimated. We assumed the epimerization consists of an initial α-carbon deprotonation, yielding the corresponding enolate, followed by reprotonation (Scheme 9). Under such conditions, deprotonation is expected to be rate determining. Calculations indicated an activation enthalpy of 16 kcal mol<sup>-1</sup> for the Et<sub>3</sub>N-catalyzed deprotonation of **10**. This value indicates a reasonably low kinetic barrier at room temperature, providing evidence for a crystallization-induced asymmetric transformation of the final product.

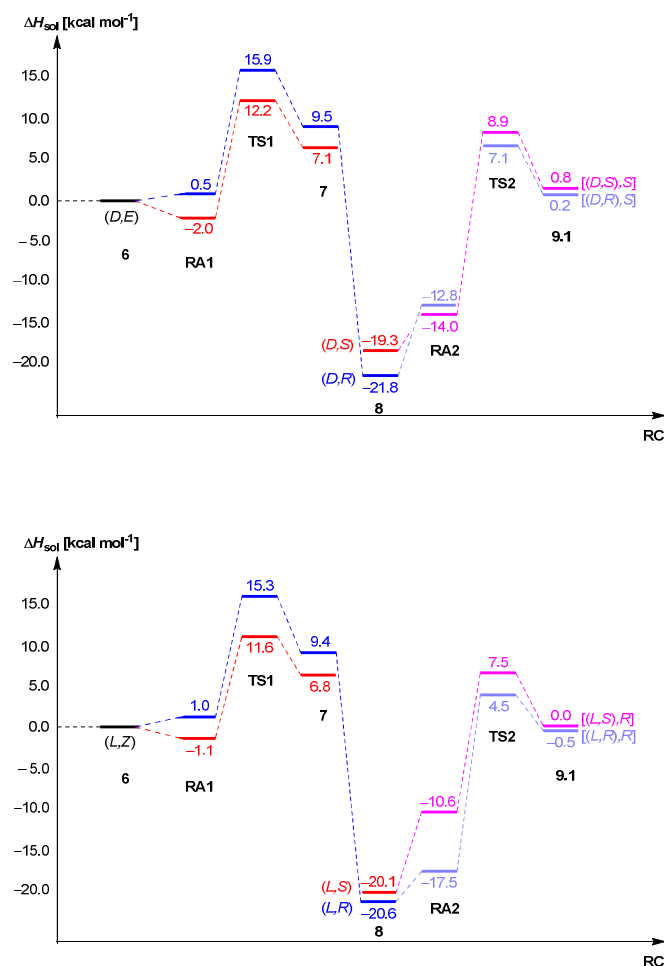
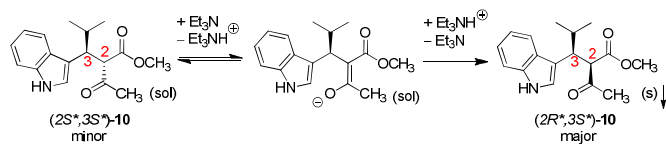


Figure 4. Calculated enthalpy profiles for the Michael reaction of indole with (*D,E*)-**6** and (*L,Z*)-**6** in dichloromethane. Two reaction paths are reported: red-magenta and blue-violet, corresponding to O-side and Cl-side attack, respectively.

Scheme 9. Et<sub>3</sub>N-catalyzed  $\alpha$ -carbon epimerization of **10**.

**Experimental evidence. Formation and reaction of **6.1** and **6.2**.** The Knoevenagel condensation of methyl acetoacetate and isobutyraldehyde was performed in the presence of 1 equiv of TiCl<sub>4</sub> and 1 equiv of Et<sub>3</sub>N in CH<sub>2</sub>Cl<sub>2</sub> at 0 °C. After 3 h, addition of 2 equiv of AgOTf (chloride scavenger) resulted into quantitative precipitation of AgCl, whose identity was confirmed by the qualitative test of solubilization with conc. aq. NH<sub>4</sub>OH. This observation indicates the dissociation of two chloride ions from titanium during the Knoevenagel condensation, and is therefore indirect evidence for the formation of adducts **6.1** and **6.2**.

In another experiment, we performed the trimolecular condensation of indole, isobutyraldehyde, and methyl acetoacetate in the presence 2 equiv of AgOTf (see Supporting Information). The scavenger was added to the reaction mixture after completion of Knoevenagel condensation and before addition of indole, so as to evaluate the scavenger influence on the Michael reaction only. Under such conditions, the condensation product **10** was isolated in 18% yield. This yield is lower than that obtained in the absence of scavenger (45%),<sup>9</sup> possibly due to complexation of silver ion by indole.<sup>71-73</sup> Nevertheless, the formation of **10** in the presence of chloride scavenger suggests that **6.1** and **6.2** are intermediates in the trimolecular condensation.<sup>71</sup>

**Formation of **8** and **9**.** Attempts to trap enolate ion **8** by methylation or benzylation using an excess (2 equiv) of methyl iodide or benzyl bromide were unsuccessful, presumably due to the complexity of reaction mixture. However, Et<sub>3</sub>N-catalyzed epimerization of the pure diastereomer (2R\*,3S\*)-**10** in CDCl<sub>3</sub> was observed by <sup>1</sup>H NMR spectroscopy. This result provides evidence for the formation of free enolate **9** and – indirectly – for its precursor **8**, which is the stable form of **9** in the presence of Ti(IV).

## Conclusions

The titanium-promoted trimolecular condensation of methyl acetoacetate, isobutyraldehyde, and indole was studied by a theoretical and experimental approach. The study revealed that titanium plays a key role in the reaction: 1) it increases the acidity of active methylene compound, allowing the easy generation of the active species (enolate); 2) it coordinates both enolate and aldehyde, promoting the aldol condensation; 3) it favors the intramolecular elimination of titanyle group with generation of the Knoevenagel adduct; 4) it increases the electrophilicity of Knoevenagel adduct by complexation; 5) it orientates the attack of indole at C <sub>$\beta$</sub>  of the Knoevenagel adduct by favoring the formation of hydrogen bonds between the indole N–H group and the titanium ligands; and 6) it stabilizes the anionic intermediate **8** by electronic delocalization towards metal ligands. In terms of electronic structure, the promoting effect of Ti(IV) can be ascribed to its electron-poor nature. The *d*<sup>0</sup> configuration and the large positive charge of Ti(IV) make this Lewis acid hard, and as such highly oxophilic.<sup>74</sup> The high diastereoselectivity of the trimolecular reaction is likely

induced by crystallization after final work-up with aqueous HCl. This study shed light on the mechanism of the trimolecular condensation and the role of metal in reaction regio- and stereochemistry, providing a model for the interpretation of analogous reactions.

## Acknowledgements

This work was carried out with support from the University ‘G. d’Annunzio’ of Chieti-Pescara and MIUR (PRIN 2010-11, prot. 2010N3T9M4). A. R. thanks the Japan Society for the Promotion of Science for providing a JSPS Invitation Fellowship for Research in Japan (FY2013).

## Notes and references

<sup>a</sup> Department of Chemistry, Osaka City University, 3-3-138 Sugimoto, Sumiyoshi-ku, 558-8585 Osaka, Japan.

<sup>b</sup> Dipartimento di Farmacia, Università ‘G. d’Annunzio’ di Chieti-Pescara, via dei Vestini 33, I-66100 Chieti, Italy.

<sup>c</sup> Institut de Chimie Moléculaire de Reims, UMR CNRS 7312, Université de Reims Champagne-Ardenne, Faculté de Pharmacie, 51 rue Cognacq-Jay, F-51096 Reims, France.

† These authors contributed equally.

Electronic Supplementary Information (ESI) available: Computational details, calculation of diastereomeric excess, experimental section, NMR spectra, and supplementary Figures, Charts, Schemes, and Tables. See DOI: 10.1039/b000000x/

1. B. B. Toure and D. G. Hall, *Chem. Rev.*, 2009, **109**, 4439-4486.
2. J. Zhu and H. Bienaymé, eds., *Multicomponent Reactions*, Wiley-VCH Verlag GmbH & Co. KGaA, 2005.
3. J. J. Müller, ed., *Science of Synthesis, Multicomponent reactions*, Thieme, 2014.
4. M. A. Mironov, *Russ. J. Gen. Chem.*, 2010, **80**, 2628-2646.
5. A. Kadam, Z. Zhang and W. Zhang, *Curr. Org. Synth.*, 2011, **8**, 295-309.
6. M. N. Khan, S. Pal, S. Karamthulla and L. H. Choudhury, *RSC Adv.*, 2014, **4**, 3732-3741.
7. C. J. O’Connor, H. S. G. Beckmann and D. R. Spring, *Chem. Soc. Rev.*, 2012, **41**, 4444-4456.
8. J. E. Biggs-Houck, A. Younai and J. T. Shaw, *Curr. Opin. Chem. Biol.*, 2010, **14**, 371-382.
9. A. Renzetti, E. Dardennes, A. Fontana, P. De Maria, J. Sapi and S. Gérard, *J. Org. Chem.*, 2008, **73**, 6824-6827.
10. S. Gérard, A. Renzetti, B. Lefevre, A. Fontana, P. De Maria and J. Sapi, *Tetrahedron*, 2010, **66**, 3065-3069.
11. A. Marrone, A. Renzetti, P. De Maria, S. Gérard, J. Sapi, A. Fontana and N. Re, *Chem. Eur. J.*, 2009, **15**, 11537-11550.
12. K. Narasaka, K. Soai, Y. Aikawa and T. Mukaiyama, *Bull. Chem. Soc. Jpn.*, 1976, **49**, 779-783.
13. D. Wang, Y. Wei and M. Shi, *Asian J. Org. Chem.*, 2013, **2**, 480-485.
14. B. Ressault, A. Jaunet, P. Geoffroy, S. Gouedranche and M. Miesch, *Org. Lett.*, 2012, **14**, 366-369.
15. R. Okuno, J.-i. Matsuo and H. Ishibashi, *Chem. Pharm. Bull.*, 2012, **60**, 793-797.
16. A. Olivella, C. Rodriguez-Esrich, F. Urpi and J. Vilarrasa, *J. Org. Chem.*, 2008, **73**, 1578-1581.
17. M. Ikonaka, *Org. Process Res. Dev.*, 2007, **11**, 495-502.



18. A. K. Ghosh and M. Shevlin, in *Modern Aldol Reactions*, ed. R. Mahrwald, Wiley-VCH Verlag GmbH, 2008, pp. 63-125.
19. Y. Yin, Q. Zhang, J. Li, S. Sun and Q. Liu, *Tetrahedron Lett.*, 2006, **47**, 6071-6074.
20. T. Hayashi, N. Tokunaga, K. Yoshida and J. W. Han, *J. Am. Chem. Soc.*, 2002, **124**, 12102-12103.
21. R. Mahrwald, *J. Prakt. Chem.*, 1999, **341**, 595-599.
22. J. Otera, Y. Fujita, N. Sakuta, M. Fujita and S. Fukuzumi, *J. Org. Chem.*, 1996, **61**, 2951-2962.
23. L. Falborg and K. A. Jorgensen, *J. Chem. Soc., Perkin Trans. 1*, 1996, 2823-2826.
24. M. Bellassoued, S. Mouelhi, P. Fromentin and A. Gonzalez, *J. Organomet. Chem.*, 2005, **690**, 2172-2179.
25. K. Yagi, T. Turitani, H. Shinokubo and K. Oshima, *Org. Lett.*, 2002, **4**, 3111-3114.
26. S. J. Brocchini and R. G. Lawton, *Tetrahedron Lett.*, 1997, **38**, 6319-6322.
27. M. Seki, T. Yamanaka, T. Miyake and H. Ohmizu, *Tetrahedron Lett.*, 1996, **37**, 5565-5568.
28. A. Bernardi, P. Dotti, G. Poli and C. Scolastico, *Tetrahedron*, 1992, **48**, 5597-5606.
29. D. A. Evans, F. Urpi, T. C. Somers, J. S. Clark and M. T. Bilodeau, *J. Am. Chem. Soc.*, 1990, **112**, 8215-8216.
30. K. Narasaka, *Org. Synth.*, 1987, **65**, 12-16.
31. M. Miyashita, T. Yanami, T. Kumazawa and A. Yoshikoshi, *J. Am. Chem. Soc.*, 1984, **106**, 2149-2156.
32. P. A. Demidov, I. A. Lavrent'ev and V. V. Potekhin, *Russ. J. Appl. Chem.*, 2012, **85**, 1676-1680.
33. S. Zari, T. Kailas, M. Kudrjashova, M. Oeren, I. Jarving, T. Tamm, M. Lopp and T. Kanger, *Beilstein J. Org. Chem.*, 2012, **8**, 1452-1457, No. 1165.
34. M. Laars, K. Ausmees, M. Uudsemaa, T. Tamm, T. Kanger and M. Lopp, *J. Org. Chem.*, 2009, **74**, 3772-3775.
35. G. Bose, V. T. Hong Nguyen, E. Ullah, S. Lahiri, H. Görls and P. Langer, *J. Org. Chem.*, 2004, **69**, 9128-9134.
36. T. C. Wabnitz, J.-Q. Yu and J. B. Spencer, *Chem. - Eur. J.*, 2004, **10**, 484-493.
37. D. C. Chatfield, A. Augsten, C. D'Cunha, E. Lewandowska and S. F. Wnuk, *Eur. J. Org. Chem.*, 2004, 313-322.
38. S. Kinoshita, H. Kinoshita, T. Iwamura, S.-I. Watanabe and T. Kataoka, *Chem. - Eur. J.*, 2003, **9**, 1496-1502.
39. C. Patel and R. B. Sunoj, *J. Org. Chem.*, 2009, **75**, 359-367.
40. M. T. Reetz and M. Von Itzstein, *J. Organomet. Chem.*, 1987, **334**, 85-90.
41. T. Rossi, C. Marchioro, A. Paio, R. J. Thomas and P. Zarrantonello, *J. Org. Chem.*, 1997, **62**, 1653-1661.
42. P. Job, *Ann. Chim. Appl.*, 1928, **9**, 113-203.
43. Z. D. Hill and P. MacCarthy, *J. Chem. Educ.*, 1986, **63**, 162-167.
44. V. M. S. Gil and N. C. Oliveira, *J. Chem. Educ.*, 1990, **67**, 473-478.
45. R. Sahai, G. L. Loper, S. H. Lin and H. Eyring, *Proc. Nat. Acad. Sci. U. S. A.*, 1974, **71**, 1499-1503.
46. R. W. Ramette, *J. Chem. Educ.*, 1963, **40**, 71-72.
47. H. E. Bent and C. L. French, *J. Am. Chem. Soc.*, 1941, **63**, 568-572.
48. D. M. Puri and R. C. Mehrotra, *J. Less-Common Met.*, 1961, **3**, 247-252.
49. P. Sobota, S. Szafert and T. Lis, *J. Organomet. Chem.*, 1993, **443**, 85-91.
50. In some cases Mulliken and NAO analyses provided slightly different results (Table S2).
51. C. B. Shinisha and R. B. Sunoj, *J. Am. Chem. Soc.*, 2010, **132**, 12319-12330.
52. R. Antonioletti, P. Bovicelli and S. Malancona, *Tetrahedron*, 2002, **58**, 589-596.
53. The predominant mechanism of electrophilic substitution at aromatic rings (including indole) is electrophilic addition-elimination, in which the intermediate carbocation undergoes loss of H<sup>+</sup> from the same carbon to which the electrophile is added (see note 54). Deprotonation of N instead of C-3 in **7** would not restore indole aromaticity and therefore can be ruled out.
54. J. Barluenga and C. Valdés, in *Modern Heterocyclic Chemistry*, Wiley-VCH Verlag GmbH & Co. KGaA, 2011, p. 380.
55. C. H. Rochester, in *Organic Chemistry - A Series of Monographs*, ed. A. T. Blomquist, Academic Press, 1970, vol. 17, p. 39.
56. E. E. Suslova, E. N. Ovchenkova and T. N. Lomova, *Tetrahedron Lett.*, 2014, **55**, 4325-4327.
57. Calculations performed at a slightly lower level of theory (see Computational details) indicated that the activation enthalpy in solution for step VII is approximately zero (-0.3 kcal mol<sup>-1</sup>). The negative sign is due to the inherent approximation of the level of theory, affecting both activation enthalpy in the gas phase (+1.56 kcal mol<sup>-1</sup>) and the implicit solvation energy difference (-1.88 kcal mol<sup>-1</sup>), whose summation yields the activation enthalpy in solution.
58. J. R. Keeffe and A. J. Kresge, in *The Chemistry of Enols*, John Wiley & Sons, New York, 2010, pp. 399-480.
59. In Figure 4, the activation enthalpy for step VIII.1 is different for each enantiomer, suggesting an erroneous e.e. ≠ 0. This difference is only due to the fact that enantiomers were evaluated in two slightly different conformations. However, each conformation can be converted into the specular one by a simple inversion operation which does not affect the related activation enthalpy. Therefore, we assumed that each enantiomer reacts through the smaller activation enthalpy available to that couple.
60. K. Yanagisawa and J. Ovenstone, *J. Phys. Chem. B*, 1999, **103**, 7781-7787.
61. C. Di Valentin, A. Tilocca, A. Selloni, T. J. Beck, A. Klust, M. Batzill, Y. Losovyj and U. Diebold, *J. Am. Chem. Soc.*, 2005, **127**, 9895-9903.
62. B. Grzmil, D. Grela and B. Kic, *Chem. Pap.*, 2008, **62**, 18-25.
63. H. Song, B. Liang, L. Lü, P. Wu and C. Li, *Int. J. Min. Met. Mater.*, 2012, **19**, 642-650.
64. E. L. Eliel, *Elements of Stereochemistry*, John Wiley & Sons, New York, 1994.
65. J. Jacques, A. Collet and S. H. Wilen, *Enantiomers, Racemates, and Resolutions*, John Wiley & Sons, New York, 1981.
66. F. Gasparrini, M. Pierini, C. Villani, P. De Maria, A. Fontana and R. Ballini, *J. Org. Chem.*, 2003, **68**, 3173-3177.
67. N. G. Anderson, *Org. Process Res. Dev.*, 2005, **9**, 800-813.
68. R. Yoshioka, *Top. Curr. Chem.*, 2007, **269**, 83-132.
69. W. H. J. Boesten, J.-P. G. Seerden, L. B. de, H. J. A. Dielemans, H. L. M. Elsenberg, B. Kaptein, H. M. Moody, R. M. Kellogg and Q. B. Broxterman, *Org. Lett.*, 2001, **3**, 1121-1124.

## Journal Name

70. P. Jakubec, P. Petráš, A. Ďuriš and D. Berkeš, *Tetrahedron: Asymmetry*, 2010, **21**, 69-74.
71. B. Bellina, I. Compagnon, L. MacAleese, F. Chirot, J. Lemoine, P. Maitre, M. Broyer, R. Antoine, A. Kulesza, R. Mitric, V. Bonacic-Koutecky and P. Dugourd, *Phys. Chem. Chem. Phys.*, 2012, **14**, 11433-11440.
72. I. O. Koshevoy, J. R. Shakirova, A. S. Melnikov, M. Haukka, S. P. Tunik and T. A. Pakkanen, *Dalton Trans.*, 2011, **40**, 7927-7933.
73. R. Antoine, T. Tabarin, M. Broyer, P. Dugourd, R. Mitric and V. Bonacic-Koutecky, *ChemPhysChem*, 2006, **7**, 524-528.
74. R. G. Pearson, *J. Am. Chem. Soc.*, 1963, **85**, 3533-3539.